Predictive Maintenance Approach in Ventricular Assist Devices: Safeguarding Against Thrombus Formation

THIAGO SANTOS[1], OSWALDO MARTINS[1], EDUARDO BOCK[1], DENNIS TOUFEN[2]
[1]Laboratory of Bioengineering and Biomaterials, Mechanical Department,
Federal Institute of Education, Science, and Technology of Sao Paulo,
Pedro Vicente Street, 625 - Caninde, Sao Paulo - SP, 01109-010,
BRAZIL

[2]Industrial Automation Department,
Federal Institute of Education, Science, and Technology of Sao Paulo,
Salgado Filho Avenue, 3501 – Vila Rio de Janeiro, Guarulhos - SP, 07115-000,
BRAZIL

Abstract: - Affecting millions in the world, cardiovascular diseases are a public health problem. Some patients are not eligible for heart transplantation. Thus, a possibility is to receive a circulatory device known as a ventricular assist device (VAD). This kind of device shows some problems, like thrombogenesis. The thrombus formation in a VAD can cause patient death, and a previous, non-invasive diagnostic is quite complex. The objective of this work is to develop an algorithm to reproduce time signals that indicate the presence and absence of a thrombus, use these signals to train an artificial neural network to classify them, and use these algorithms in a predictive algorithm for early thrombus detection. The results show that it was possible to detect the thrombus formation in its early stages, but the noise level interferes with the accuracy of the ANN, especially when signals in the time domain are used.

Key-Words: - Ventricular assist device, thrombus, artificial neural network, signal analysis, predictive maintenance, artificial intelligence, machine learning.

Received: March 8, 2023. Revised: November 5, 2023. Accepted: December 7, 2023. Published: January 8, 2024.

1 Introduction

Affecting millions of people around the world, cardiovascular diseases (CD) are responsible for the first cause of death and hospitalization, making them a serious public health problem, [1]. Many patients suffering from Congestive Heart Failure (CHF) need heart transplantation, although many of them will die until they receive the donated heart, [2]. To minimize this death rate, some of them receive a circulatory device known as a ventricular assist device (VAD), [3].

The VADs are established as a good therapy for patients with end-stage heart failure, [2]. The function of VAD is to replace the mechanical work of the left or right ventricles, [4]. The VAD is a pump with a motor, controller, outflow graft, drive line cable, and batteries, as shown in Figure 1, [5].

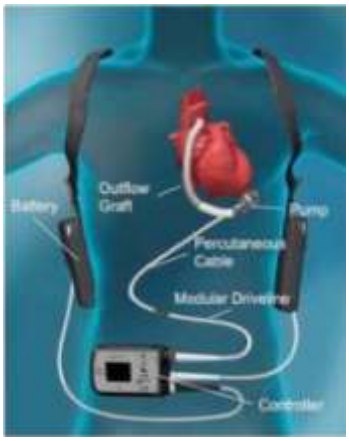

Fig. 1: VAD with batteries, controller, and peripheral systems. Adapted from, [5]

2 Thrombosis on VADs

The VADs still show some problems in hemocompatibility, among them thrombogenesis, which is a kind of natural coagulation when blood is

exposed to any surface not fully covered by endothelium, blood flow inside the pump, and others, [6]. One of the most common therapies to avoid thrombus formation in VAD is the prescription of anticoagulants that will dissolve the thrombus, [7]. However, this therapy will be effective only if the patient starts it in the first stages of thrombosis, [8]. Figure 2 shows a VAD with a thrombus formation that has been removed from a 56-year-old patient. According to the authors, the thrombus was blocking around 95% of the inlet cannula, [9].

Fig. 2: Thrombus formation in a removed VAD. Adapted from, [9]

The thrombus formation can result in VAD disability or even cause the patient's death, [3], [10]. Immediate action is necessary, but in the current scenario is indecisive about which treatment needs to be carried out, [11]. The thrombus formation and its consequent release into the patient's body is one of the main causes of death in patients implanted with VAD, [12]. A VAD controller that diagnoses the appearance of a thrombus before its release can be vital to a patient's life, and several studies are being conducted with this objective, [8], [13].

3 Signal Analysis

Based on data from an experimental study that performed tests with artificial thrombus in a pump prototype, the objective of this work is to develop a Python language algorithm to reproduce simulated signals obtained by that study that indicate the disturbances caused by the presence of artificial thrombus adhered in three different regions of the pump, then use these signals to train an artificial neural network (ANN) to taxonomy them, check its robustness for noise interference, and later use this ANN in a predictive algorithm to check the probability of absence and presence of thrombus.

3.1 Vibration Analysis

The theoretical basis for the reconstruction and analysis algorithms used in this work is classical vibration theory, which we will briefly present here. The classic model of translational forced vibration with viscous damping is described by Equation 1, [14].

$$m\ddot{x} + c\dot{x} + kx = F_0 \sin(\omega t) \tag{1}$$

where x is the linear displacement, k is the spring constant or stiffness, c is the damping coefficient and $F_0 \sin(\omega t)$ is the excitation force.

Defining, the natural frequency as

$$\omega_n = \sqrt{\frac{k}{m}} \tag{2}$$

and the fraction of critical damping as

$$\zeta = \frac{c}{2m\omega_n} \tag{3}$$

The acceleration is calculated by

$$\ddot{x} = -\frac{m}{F_0}\left(\frac{\omega}{\omega_n}\right)^2 R_d \sin(\omega t - \theta) \tag{4}$$

θ is the acceleration phase and Rd is a dimensionless response factor:

$$R_d = \frac{1}{\sqrt{\left(1-\omega^2/\omega_n^2\right)^2 + (2\zeta\omega/\omega_n)^2}} \tag{5}$$

For a non-harmonic excitation force, like that observed for the thrombus presence in VADs, [15], Fourier analysis is used to break it down into its harmonic components as a function of frequency. Each of these components can have its acceleration solution calculated by Equation 4. Assuming the system is linear, the superposition principle allows the summation of the solutions from multiple components to obtain the total expected acceleration.

3.1 Work reference

The [15], presents an in vitro study where the vibrational signal analysis, obtained with Microelectromechanical Systems (MEMS) accelerometers, was used to identify disturbances or stimulations that indicate dynamic changes on the pump's rotor when the thrombi adhere or if there is wear on the rotating elements. The Fast Fourier Transform (FFT) is used to characterize signal components in the frequency domain. Figure 3 shows the experimental set-up used by the authors

for their study, and Figure 4 shows the areas where the thrombosis was simulated. The material used to simulate the thrombus had a density of 0.97 g/cm2, and the liquid used to simulate the circulatory system was water, [15].

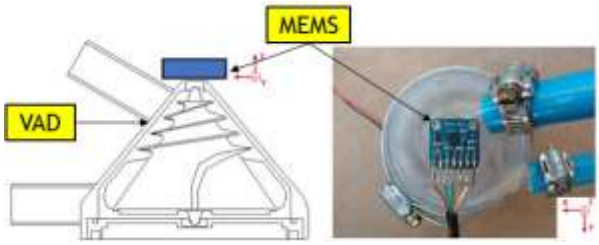

Fig. 3: Experimental set-up. Adapted from, [15]

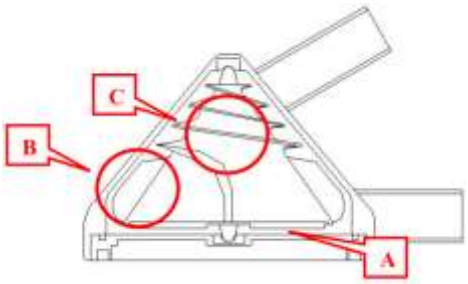

Fig. 4: Areas where the thrombus was simulated

According to the results shown by the authors, the MEMS could detect disturbances caused by thrombus formation. In that work, it is informed that the presence or absence of a thrombus is characterized by the occurrence of peaks at determinate frequencies. The red arrow in the graph of the Figure 5 spectrum indicates an imbalance caused by thrombus presence. For example, the peak next to the 145 Hz frequency indicates an unbalance on the rotor caused by the thrombus presence at the rotor's base.

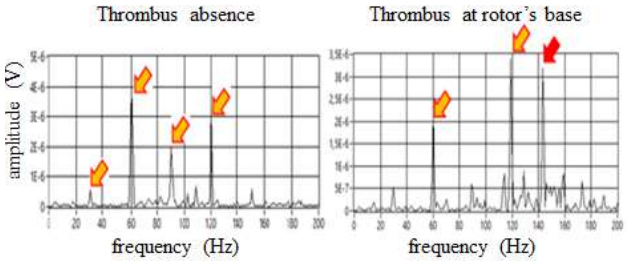

Fig. 5: Frequency spectrum patterns for thrombus absence and presence at rotor's base. Adapted from, [15]

4 Methodology

This work was divided into four main methodologies: 1 - creation of a synthetic dataset that reproduces the time signals obtained by, [15]; 2 - creation of an algorithm to simulate the evolution of thrombus formation and evaluate it by the wavelet analysis; 3 - creation of ANN algorithm to classify the signals in the synthetic dataset; 4 - creation of a predictive algorithm, using the ANN to check the probability of thrombus absence and presence.

4.1 Time Signals Reconstruction

The results from [15], were used to create the Signals Reconstruction Algorithm (SRA), which was used to create a synthetic dataset in Python language of voltage in the time and frequency domain. The graphs shown in that work provide data such as the maximum voltage amplitude for each frequency peak, noise, and sampling rate. With these data, cosine signals were used to create a clean signal with the same amplitudes. After modeling the "clean signal," background noise was added with a Gaussian distribution, represented by Equation 6, to get a more realistic synthetic dataset simulated signal like the real one,

$$s(t) = A \cdot \cos(2\pi f t + \emptyset) + n(t) \quad (6)$$

where s(t) is the signal as a function of time, A is the amplitude of the signal, f is the frequency of the signal, t is time, $\emptyset$ is the phase of the signal and n(t) is the Gaussian noise component.

The Fourier transform, computed using the fast Fourier transform (FFT) in combination with a window function, was applied to each one of those created signals, then the results were squared to get the power spectrum value, and these results were plotted.

This methodology was applied to all the results of the work referenced in this section. The algorithm sequence is presented below.

1. **Parameters Definition**: The process starts by defining crucial parameters such as the sampling rate, data acquisition time, and background noise amplitude, along with creating a time vector.
2. **Noise Generation**: A vector of Gaussian noise is generated, representing the noise component to be added later to the signals.
3. **Signal Generation Without Thrombus**: A correction factor is defined, and a signal vector without thrombus is created by adding sine waves of different frequencies based on defined amplitudes.
4. **Calculation of Power Spectrum Without Thrombus**: The "*signal.welch"* function is used to calculate the power spectrum of the signal without thrombus.

5. **Signal Generation with Thrombus at the base, vanes, and spiral**: The process from step 3 is repeated to generate signals with thrombus at different parts of the VAD, adjusting amplitudes and specific correction factors.
6. **Graph Creation**: Graphs are plotted to visualize the signals and power spectra, organized into multiple subplots for each signal type.

4.2 Wavelet Analysis

This work step involves developing the Changing State Algorithm (CSA) to simulate the signal's state transition, reflecting thrombus formation evolution. Leveraging data from the SRA and wavelet analysis, [16], the algorithm sequence is outlined. Figure 6 visually represents the transition between two different signals.

1. **Importation of Signals**: Signals generated by the SRA are initially imported.
2. **Simulation of State Transition**: The code enters a loop simulating a state transition over a period *ti*. The loop increments or decrements the amplitudes of specific frequencies, simulating a transition from the initial state to the final state.
3. **Creation of the Complete Signal**: The signal is constructed by summing the sinusoidal components of specified frequencies over time and adding previously generated noise.
4. **Analysis and Visualization of Power Spectrum**: The code creates a spectrogram using the *pcolormesh* function to plot the magnitude of the Continuous Wavelet Transform against time and frequency. Default settings were used for both commands [16].
5. **Display of Results**: The graphical results are plotted.

In the sequence above, the period *ti* can be interpreted as a time value, representing days, weeks, months, etc. The higher the value of *ti*, the smoother the curve representing the state change. The value used for *ti* was 1000. In plotting the results, the argument *cmap=jet* was used, representing a color palette with smooth transitions from blue to red. Thus, the higher the amplitude, the redder the coloration presented.

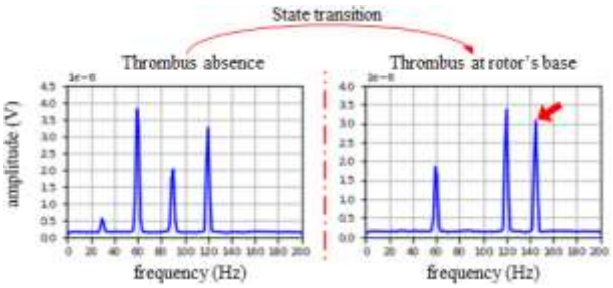

Fig. 6: Transition from a thrombus-free state to the presence of a thrombus at the base of the rotor.

4.3 Artificial Neural Network

The ANN is a computational model of Machine Learning inspired by the complex functionality of the human brain, where billions of neurons process information in parallel, [17]. An ANN is made up of three main layers: the input layer, the hidden layer, and the output layer. These layers are interconnected by non-linear nodes, forming a neural network of interconnections. In an ANN, each input is multiplied by a synaptic weight (a weighting factor), and each neuron has its synaptic weight to be added, [18]. The activation potential is calculated by adding the bias to the product of the inputs and their corresponding synaptic weights. This activation potential is then applied to an activation function, resulting in the neuron's output, [17]. In summary, the output of a neuron can be represented by Equation 7, where y represents the neuron output, σ is the activation function, n is the number of inputs, w_i are the synaptic weights associated with the inputs, x_i are the input values, and θ is the neuron bias

$$y = \sigma\left(\sum_{i=1}^{n} w_i x_i + \theta\right) \quad (7)$$

4.3.1 Implemented Artificial Neural Network

This algorithm takes the data and classifies it based on its characteristics. Figure 7 shows an example of how the ANN algorithm works.

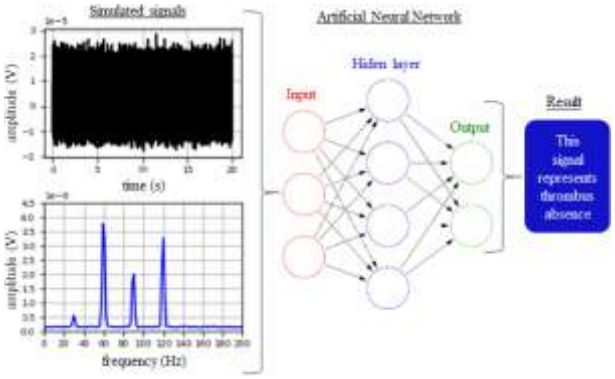

Fig. 7: ANN classifying the synthetic signals

The dataset obtained by the SRA was processed by a fully connected Feed Forward ANN architecture. Four classes and four labels for data classification (Table 1) were chosen. To train and test the ANN, the dataset was divided as follows: 70% for training and 30% for validation. This procedure was applied to both types of obtained signals – time and frequency domains. The created has 3 layers, and its characteristics are as follows:

- Layer 1 – Type dense, number of neurons = 26, activation function = "relu".
- Layer 2 – Type dense, number of neurons = 128, activation function – "relu".
- Layer 3 – Type dense, number of neurons = 4, activation function – "SoftMax".

The number of epochs was 4000 and the optimizer used to reduce overall loss was, [19]. The metric used to check performance was accuracy. To assess the noise sensitivity of the ANN, it was tested and trained with signals from both the time and frequency domains, with the background noise being gradually increased. The best-performing ANNs in terms of accuracy sensitivity will be used in the predictive algorithm.

Table 1. Dataset created to classify different VAD working scenarios

Label	Class
0	Thrombus absence
1	Thrombus at rotor's base
2	Thrombus at rotor's vanes
3	Thrombus at rotor's spiral

4.4 Predictive Algorithm

This model utilizes the best ANNs with the dataset generated by the SRA to predict the probability of thrombus absence or presence in a specific timeframe. The objective is to merge signals representing the absence of a thrombus with signals indicating the presence of a thrombus, simulating the transition of signals from "without thrombus" to "with thrombus" over time. This model provides a comprehensive analysis of the temporal variations in the probabilities of thrombus presence or absence and was designed to better simulate real-life applications.

The code initiates a loop that varies the starting point of the region, indicating the absence of a thrombus, adjacent to the region indicating thrombus presence. In each iteration, the thrombus probability is calculated for this evolving data range, and the calculated probabilities are stored. At the end of the iterations, they are visually represented in a line graph, illustrating how the probabilities evolve. This allows for a detailed analysis of changes as the data range varies. The algorithm sequence is presented below.

1. **Loading the pre-trained ANN**: The algorithm loads the ANN from the file where it was saved using the "TensorFlow" library.
2. **Calculation Loop**: The code enters a loop that calculates tracks of the dataset with different starting points for region 1 (without thrombus) and varies the start of region 2 (with thrombus). At the loop's initiation, the track contains only data from region 1. As the iterations progress, region 1 decreases at the same rate as region 2 increases. The total number of iterations is defined by the size of the matrix previously pre-processed by the ANN algorithm.
3. **Average Calculation**: The code calculates the average of all rows in the data range.
4. **Reshape the Data for the ANN**: The average data is reshaped to have the appropriate format to be used as input for the ANN.
5. **ANN predictions**: Predictions are obtained by applying the implemented ANN to the simple average data. This algorithm calculates the probability of thrombus presence or absence based on the information in the data track.
6. **Probability Calculation**: The probabilities computed by the ANN are converted into percentage values representing the likelihood of thrombus presence or absence.
7. **Probability Storage**: The calculated probabilities are stored in two separate lists: one for thrombus absence probability and the other for thrombus presence probability, for recording and analysis purposes.
8. **Chart Plotting**: Finally, the code generates a line chart using the matplotlib library to display the evolution of probabilities over iterations. The chart shows the probabilities of "Prob. Without Thrombus" and "Prob. With Thrombus" on the vertical axis in percentage and the iterations on the horizontal axis.

5 Results

In this section, we will present the results obtained by the SRA, the CSA, the results obtained by the ANNs in classifying the reproduced signals, and their performance with increased background noise. Finally, we will present the results of the predictive

algorithms. To facilitate comprehension, these results have been divided into the following four subsections.

5.1 Signal Reconstruction Algorithm

The spectrum pattern representing the absence of thrombi is characterized by peaks at the fundamental frequency of 30 Hz and its respective harmonics (60, 90, and 120 Hz). The presence of a thrombus at the base is identified by a peak near the frequency of 140 Hz. In the case of thrombus presence at the vanes, an increase in amplitudes at frequencies of 90 and 120 Hz and the appearance of peaks at frequencies of 150 and 180 Hz indicate this anomaly. The elevation in amplitudes at frequencies of 90 and 120 Hz indicates the presence of a thrombus in the rotor spiral.

5.2 Changing State Algorithm

Figure 8 shows the spectrograms from CSA for the three thrombus positions studied. Figure 8 (a) displays the time series changing from the absence to the presence of a thrombus at the rotor's base. From a certain point onward, it was possible to observe that the region associated with the frequency of 140 Hz became visible on the scale. This gradual change in coloration indicates a progressive increase in the amplitude of this frequency, directly related to the appearance of the thrombus at the rotor's base. At a certain moment, the areas corresponding to the frequencies of 90 and 120 Hz began to become less visible. The spectrograms of the other two thrombus positions, the rotor's vanes and the rotor's spiral are presented in Figure 8 (b) and (c), respectively. In both cases, we observe an intense peak at 90Hz growing with time. For the thrombus in the rotor's vane, Figure 8 (b), we observe a growing doublet at 125 and 150 Hz and for the thrombus in the rotor's spiral, Figure 8 (c), just a peak in 125 Hz is observed. The behavior of these two signals follows what is expected, showing a smooth transition between the peak of thrombus absence and presence.

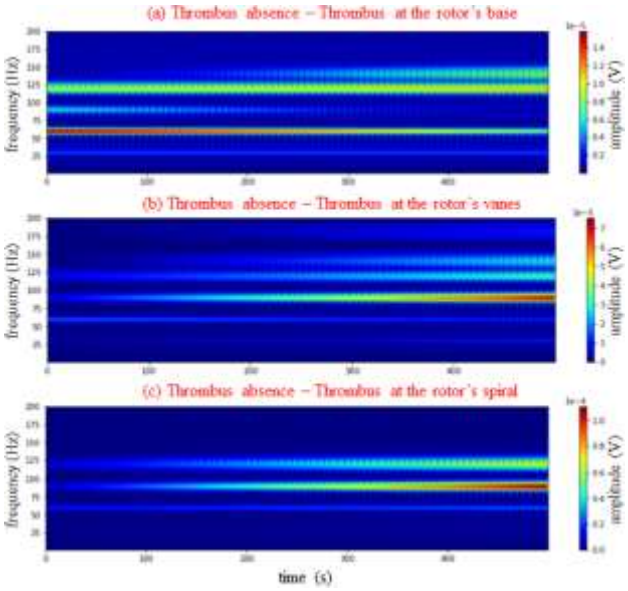

Fig. 8: Plotted results from the CSA for all working states

5.3 Implemented Artificial Neural Network

With very low noise (A = 1e-6), the ANN obtained an average accuracy of around 100% for classifying each of the signals. It was observed that, in all scenarios, as the background noise level increases, the mean accuracy decreases. A trendline was adjusted to quantify the decrease in accuracy with noise amplitude. It was noticed that the angular coefficient (α) of the trendline in frequency domain signals (αf = -0.019) is smaller than in time domain signals (αf = -0.061). Figure 9 shows the influence of noise on ANN accuracy analysis for both time and frequency domains.

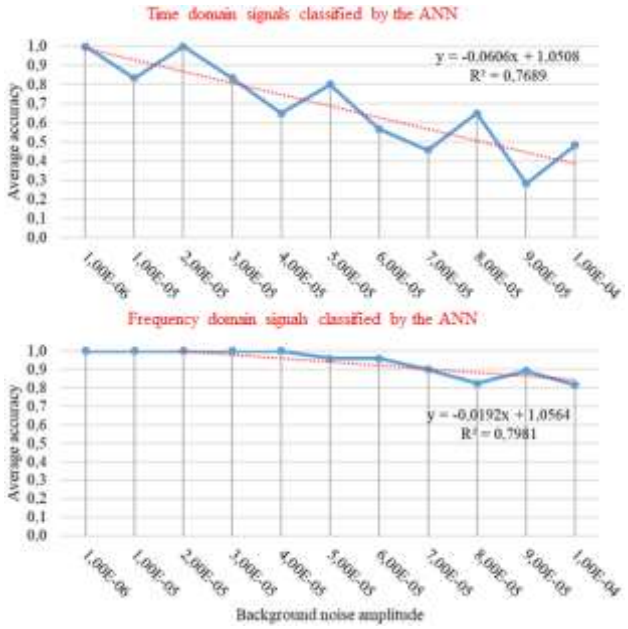

Fig. 9: ANNs performance for each kind of signal

5.4 Predictive Algorithm

To demonstrate the capability of the ANN to predict thrombus formation with a small frequency signature, the output probabilities are presented in Figure 10 for three thrombus positions. In all scenarios, illustrated throughout the iterations, where the iterations represent the degree of mixing of signals with the absence and presence of thrombus, the probabilities of thrombus absence and presence vary. As expected, the probabilities always start with 100% for thrombus absence. With the increase in mixing, they converge to around 50% when approximately half of each signal type is being analyzed. After reaching this equilibrium point, the curves begin to diverge, reaching values of 0% for thrombus absence and 100% for thrombus presence when about 30% of the signals correspond to thrombus absence, and the remaining 70% are signals of thrombus presence.

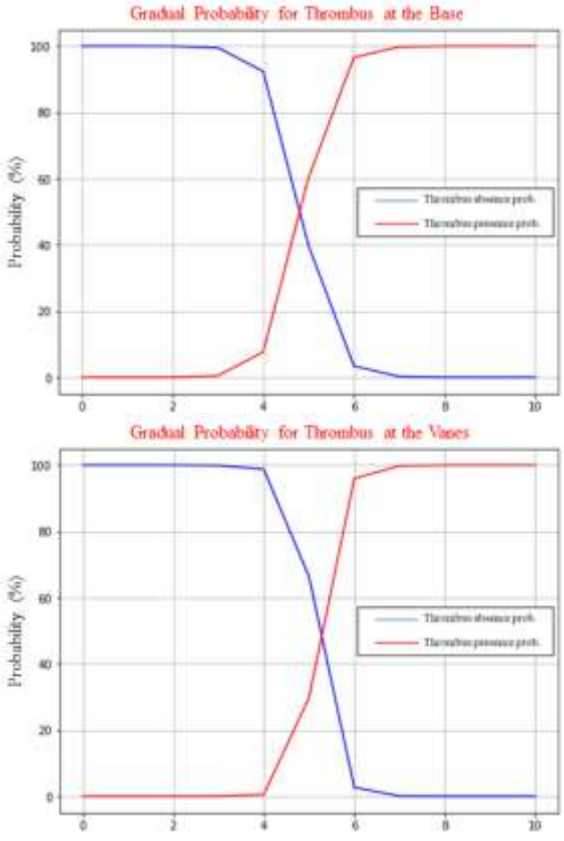

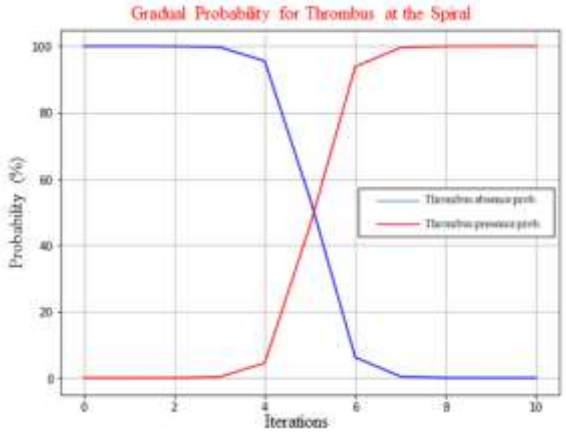

Fig. 10: Predictive analysis over the time

6 Conclusion

This study investigated the application of signal processing and machine learning algorithms for the detection of thrombi in VADs under different operating conditions. The analysis covered signal reconstruction techniques, signal analysis, classification by ANNs, and their application in a predictive algorithm. Frequency analysis highlighted specific characteristics for each scenario, with some frequencies indicating normality and the absence of a thrombus, while others indicated the presence of a thrombus, signaling anomalies and imbalances in the rotor.

A signal made by mixing signals with and without a thrombus was verified using wavelet analysis to represent how thrombus formation might develop over time, indicating that at a certain point, the signs indicating the presence of a thrombus become measurable. Classification analyses were carried out using ANNs, considering data in the time domain and the frequency domain.

Overall, frequency domain signals demonstrated superiority to time domain signals in terms of sensitivity to disturbances caused by noise, although the frequency domain requires greater computational effort to pre-process the measured signals. The frequency domain signals were used to carry out predictive analyses to calculate the probabilities of the presence or absence of thrombi in various VAD operating scenarios, including situations of total absence or presence of thrombi, as well as the variable combination of these signals over time. It was found that the probabilities varied significantly as the proportions of thrombus presence and absence data changed.

Therefore, the results of this study, especially those obtained by the predictive algorithm, contribute to the further development of a smart

pump, where more effective monitoring and control systems can be incorporated into VADs, making them more efficient, as well as suggesting the feasibility of implementing prescriptive maintenance strategies. By analyzing the data, the device itself can indicate to the patient or physician when and what should be done. It is important to note that the results of this study were obtained using only one VAD model and cannot yet be generalized.

Acknowledgement:

Special thanks to the Laboratory of Bioengineering and Biomaterials crew and the Federal Institute of Education, Science and Technology of São Paulo for their support throughout the research process.

References:

[1] G. Renugadevi, G. Asha Priya, B. Dhivyaa Sankari, and R. Gowthamani, 'Predicting heart disease using hybrid machine learning model', *J Phys Conf Ser*, vol. 1916, no. 1, 2021, doi: 10.1088/1742-6596/1916/1/012208.

[2] J. N. Heaton, S. Singh, M. Li, and S. Vallabhajosyula, 'Adverse events with HeartMate-3 Left ventricular assist device: Results from the Manufacturer and User Facility Device Experience (MAUDE) database', *Indian Heart Journal*, vol. 73, no. 6, pp. 765–767, 2021, doi: 10.1016/j.ihj.2021.10.008.

[3] J. I. Glitza, F. Müller-von Aschwege, M. Eichelberg, N. Reiss, T. Schmidt, C. Feldmann, R. Wendl, J. D. Schmitto, and A. Hein, 'Advanced telemonitoring of Left Ventricular Assist Device patients for the early detection of thrombosis', *Journal of Network and Computer Applications*, vol. 118, no. May, pp. 74–82, 2018.

[4] G. Malone, G. Abdelsayed, F. Bligh, F. Al Qattan, S. Syed, P. Varatharajullu, A. Msellati, D. Mwipatayi, M. Azhar, A. Malone, S. H. Fatimi, C. Conway, and A. Hameed, 'Advancements in left ventricular assist devices to prevent pump thrombosis and blood coagulopathy', *J Anat*, vol. 242, no. 1, pp. 29–49, 2023, doi: 10.1111/joa.13675.

[5] M. Barboza, F. Junqueira, E. Bock, T. Leão, J. Dias, J. Dias, M. Pessoa, J. R. Souza, and D. dos Santos, 'Ventricular Assist Device in Health 4.0 Context', *IFIP Adv Inf Commun Technol*, vol. 577, pp. 347–354, 2020.

[6] K. Salaunkey, J. Parameshwar, K. Valchanov, and A. Vuylsteke, *Mechanical support for heart failure 2C04 3C00*, vol. 14, no. 3. 2013. doi: 10.1177/175114371301400309.

[7] A. I. Fiorelli, J. de Lima, O. Junior, H. B. Coelho, and D. Cristo, 'Mechanical circulatory support : why and when', vol. 87, no. 1, pp. 1–15, 2008.

[8] U. P. Jorde, K. D. Aaronson, S. S. Najjar, F. D. Pagani, C. Hayward, D. Zimpfer, T. Schlöglhofer, D. T. Pham, D. J. Goldstein, K. Leadley, M. J. Chow, M. C. Brown, and N. Uriel, 'Identification and Management of Pump Thrombus in the HeartWare Left Ventricular Assist Device System: A Novel Approach Using Log File Analysis', *JACC Heart Fail*, vol. 3, no. 11, pp. 849–856, 2015.

[9] F. Ortiz and T. Thenappan, 'Low Flow Alarm in a Patient With Left Ventricular Assist Device: What Went Wrong?', *Journal of the American College of Cardiology*, vol. 73, no. 9, p. 2194, 2019, doi: 10.1016/s0735-1097(19)32800-1.

[10] E. J. Molina, P. Shah, M. S. Kiernan, W. K. Cornwell, H. Copeland, K. Takeda, F. G. Fernandez, V. Badhwar, R. H. Habib, J. P. Jacobs, D. Koehl, J. K. Kirklin, F. D. Pagani, and J. A. Cowger, 'The Society of Thoracic Surgeons Intermacs 2020 Annual Report', *Annals of Thoracic Surgery*, vol. 111, no. 3, pp. 778–792, 2021.

[11] T. Gyoten, M. Morshuis, S. V. Rojas, M. A. Deutsch, R. Schramm, J. F. Gummert, and H. Fox, 'Identification of characteristics, risk factors, and predictors of recurrent LVAD thrombosis: conditions in HeartWare devices', *Journal of Artificial Organs*, vol. 24, no. 2, pp. 173–181, 2021, doi: 10.1007/s10047-020-01228-2.

[12] A. L. Meyer, C. Kuehn, J. Weidemann, D. Malehsa, C. Bara, S. Fischer, A. Haverich, and M. Strüber, 'Thrombus formation in a HeartMate II left ventricular assist device', *Journal of Thoracic and Cardiovascular Surgery*, vol. 135, no. 1, pp. 203–204, 2008, doi: 10.1016/j.jtcvs.2007.08.048.

[13] D. J. Goldstein, R. John, C. Salerno, S. Silvestry, and N. Moazami, 'Algorithm for the diagnosis and management of suspected pump thrombus', *Journal of Heart and Lung*

Transplantation, vol. 32, no. 7, pp. 667–670, 2013, doi: 10.1016/j.healun.2013.05.002.

[14] T. D. Rossing, *Shock and Vibration Handbook , 2nd ed.* , vol. 45, no. 7. 1977. doi: 10.1119/1.10796.

[15] S. Neto, S. Sobrinho, C. Costa, T. Leão, S. Senra, E. Bock, G. Santos, S. Souza, M. Silva, C. Frajuca, and M. Souza, 'Investigation of MEMS as accelerometer sensor in an Implantable Centrifugal Blood Pump prototype', *Journal of the Brazilian Society of Mechanical Sciences and Engineering*, vol. 42, no. 9, pp. 1–10, 2020.

[16] T. Guo, T. Zhang, E. Lim, M. Lopez-Benitez, F. Ma, and L. Yu, 'A Review of Wavelet Analysis and Its Applications: Challenges and Opportunities', *IEEE Access*, vol. 10, pp. 58869–58903, 2022, doi: 10.1109/ACCESS.2022.3179517.

[17] G. M. Khan, 'Artificial neural network (ANNs)', *Studies in Computational Intelligence*, vol. 725, pp. 39–55, 2018, doi: 10.1007/978-3-319-67466-7_4.

[18] S. Biswal and G. R. Sabareesh, 'Design and development of a wind turbine test rig for condition monitoring studies', *2015 International Conference on Industrial Instrumentation and Control, ICIC 2015*, no. Icic, pp. 891–896, 2015, doi: 10.1109/IIC.2015.7150869.

[19] D. P. Kingma and J. L. Ba, 'Adam: A method for stochastic optimization', *3rd International Conference on Learning Representations, ICLR 2015 - Conference Track Proceedings*, pp. 1–15, 2015.

Contribution of Individual Authors to the Creation of a Scientific Article (Ghostwriting Policy)

- Thiago Santos was responsible for the research and algorithm creation and implementation.
- Oswaldo Martins was responsible for double-checking the results and paper review.
- Dennis Toufen and Eduardo Bock were responsible for supporting the algorithm's creation and paper review.

Sources of Funding for Research Presented in a Scientific Article or Scientific Article Itself

No funding was received for conducting this study.

Conflict of Interest

The authors have no conflicts of interest to declare.